Nuclear Instruments and Methods in Physics Research A 848 (2017) 106–108

Contents lists available at ScienceDirect

Nuclear Instruments and Methods in Physics Research A

journal homepage: www.elsevier.com/locate/nima

Technical notes

Detection of charged particles with a methylammonium lead tribromide perovskite single crystal

Qiang Xu[a], Haotong Wei[b], Wei Wei[b], William Chuirazzi[a], Dylan DeSantis[a], Jinsong Huang[b,*], Lei Cao[a,**]

[a] Nuclear Engineering Program, Department of Mechanical and Aerospace Engineering, The Ohio State University, Columbus, Ohio 43210, USA
[b] Department of Mechanical and Materials Engineering, University of Nebraska-Lincoln, Lincoln, Nebraska 68588, USA

ARTICLE INFO

Keywords:
Alpha-particle detection
Methylammonium lead tribromide perovskite single crystal
Radiation detection
Charge transport

ABSTRACT

Methylammonium lead tribromide ($MAPbBr_3$) perovskite crystals have attracted significant attention due to their attractive performance in various optoelectronic applications such as solar cells, light-emitting devices, photodetectors, and recently in X-ray detectors. In this study, we demonstrate a possible use of perovskite-based devices for detection of charged particles (which can be applied in basic scientific research, health physics, and environmental analysis) and investigate the mechanism of fundamental charge transport inside perovskite crystals. It was found that inexpensive $MAPbBr_3$ single crystals could be used for measuring the energy spectrum of charged particles through direct collection of the produced charge. After fitting the plot of the centroid peak position versus voltage with the Hecht equation for single-polarity charge transport, the obtained hole mobility-lifetime product was in the range of $(0.4–1.6)\times10^{-3}$ cm^2/V.

Most conventional radiation detectors are either semiconductors (such as Si or Ge) or scintillators (such as NaI) and utilize two different detection methods. One method is based on converting the incident radiation directly to electron-hole pairs, while the other method allows recombination of the created charge carriers and emission of UV–vis photons, which can be detected by a highly sensitive photomultiplier tube or a photodiode [1]. The conventional detectors are characterized by either low energy resolution, or high manufacturing costs, or a narrow range of the operational temperature [2,3]. Although multiple attempts have been made in the past to develop alternative detector materials such as CdZnTe [4], HgI [5], and TlBr [6], significant efforts are still required on reducing the manufacturing costs while maintaining a high detection efficiency and a competitive energy resolution. Owing to the high charge carrier mobility, long diffusion length of tens of micrometers, and low trap density of 10^9 cm^{-3} [7,8], methylammonium lead tribromide ($MAPbBr_3$) perovskite single crystals have been widely used in various optoelectronic applications such as photovoltaic cells [9,10], light-emitting diodes (LEDs) [11,12], and photodetectors [13]. Usually, the materials employed in solar cells or LEDs can also be used for manufacturing X-ray and gamma ray detectors due to their good electronic properties. Hence, highly sensitive and inexpensive $MAPbBr_3$ perovskite crystals with a high density of 3.7 g/cm^3 can be potentially utilized for this purpose [14–18]. In this work, a resistor-type radiation detector with the metal-semiconductor-metal (MSM) structure has been fabricated and subsequently tested by performing alpha spectrum measurements, while its response to gamma rays will be reported in future studies. After applying a high voltage, the electron-hole pairs produced by incident alpha particles become separated and collected by two metal contacts to form an energy spectrum. The energy spectrum of the alpha particles emitted from a 0.8 μCi ^{241}Am source was measured using $MAPbBr_3$ single crystals operating as direct band-gap semiconductors, and the related hole mobility-lifetime product was calculated via the Hecht equation. The obtained results demonstrate that $MAPbBr_3$ single crystals are capable of detecting energy-resolved charged particles.

$MAPbBr_3$ single crystals were grown through a solution process based on the anti-solvent method [18]. In particular, 0.64 M of $PbBr_2$ and 0.8 M of MABr were dissolved in 5 mL of N,N-dimethylformamide (DMF) inside a 20 mL vial; as a result, the molar ratio of $PbBr_2$ to MABr was equal to 0.8. The vial was then sealed with foil, which contained a small hole to allow slow penetration of dichloromethane (DCM) anti-solvent vapor. The designed sandwich structure of the radiation detector fabricated from a $MAPbBr_3$ single crystal is depicted in Fig. 1a (the utilized crystal size was about 5 mm×5 mm ×2 mm). A Cr cathode electrode with a thickness of 20 nm and an anode electrode containing 20 nm thick C_{60}, 8 nm thick bathocuproine (BCP), and

* Corresponding author at: Department of Mechnical and Materials Engineering, University of Nebraska-Lincoln, Lincoln, Nebraska 68588, USA.
** Corresponding author. Nuclear Engineering Program, Department of Mechanical and Aerospace Engineering, The Ohio State University, Columbus, Ohio 43210, USA.
E-mail addresses: jhuang2@unl.edu (J. Huang), cao.152@osu.edu (L. Cao).

http://dx.doi.org/10.1016/j.nima.2016.12.062
Received 3 December 2016; Received in revised form 18 December 2016; Accepted 30 December 2016
Available online 30 December 2016

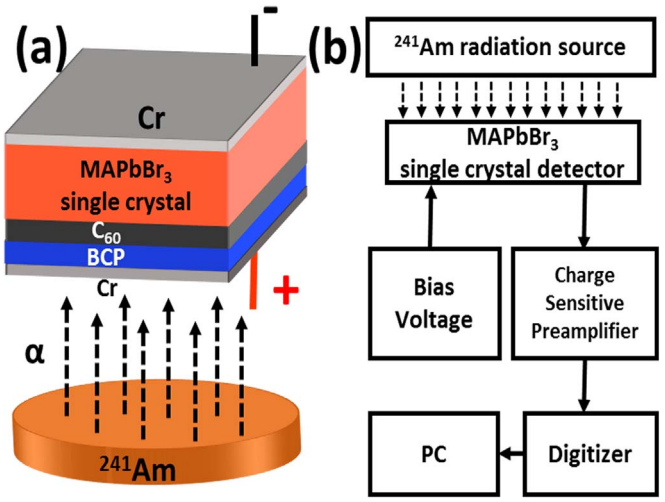

Fig. 1. (a) A schematic of the $MAPbBr_3$ single-crystal radiation detector, which contains BCP and C_{60} layers for passivation and electron extraction. (b) A flow chart describing the general structure of a digitizer-based spectroscopic system.

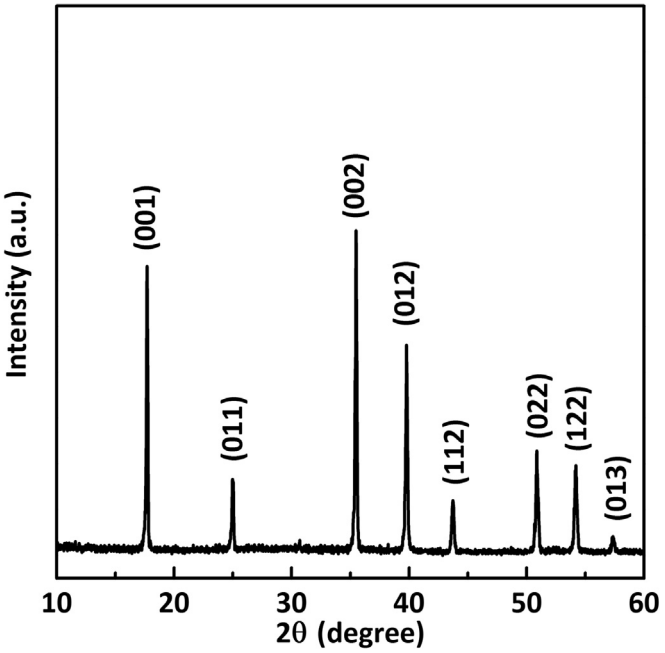

Fig. 2. An XRD pattern recorded for a powdered $MAPbBr_3$ sample.

20 nm thick Cr layers were deposited on two opposite surfaces of the $MAPbBr_3$ single crystal via thermal evaporation (here the BCP and C_{60} layers were used for passivation and electron extraction). The experimental apparatus utilized for testing the produced $MAPbBr_3$ single crystal radiation detector is schematically described in Fig. 1b (it is connected to a digital spectroscopic system consisting of a charge sensitive preamplifier and a CAEN digitizer). The testing procedure was conducted inside an Al chamber, which was completely isolated from light and electromagnetic radiation to reduce the measurement noise.

Powder X-ray diffraction (XRD) measurements were conducted to investigate the crystalline properties of $MAPbBr_3$ single crystals using a Rigaku D/Max-B X-ray diffractometer with a conventional Co target tube operated at a voltage of 40 kV and current of 30 mA. The obtained XRD pattern (Fig. 2) indicates that the $MAPbBr_3$ single crystal possesses a cubic structure of high quality.

The electrical properties of the fabricated $MAPbBr_3$ single crystal detector were investigated by measuring its current–voltage (I–V) characteristics at room temperature using a Keithley multimeter with a

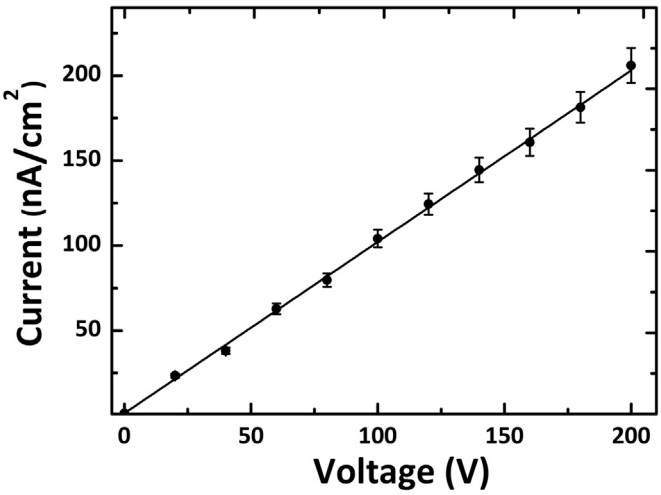

Fig. 3. An I–V characteristic curve obtained for the $MAPbBr_3$ single crystal.

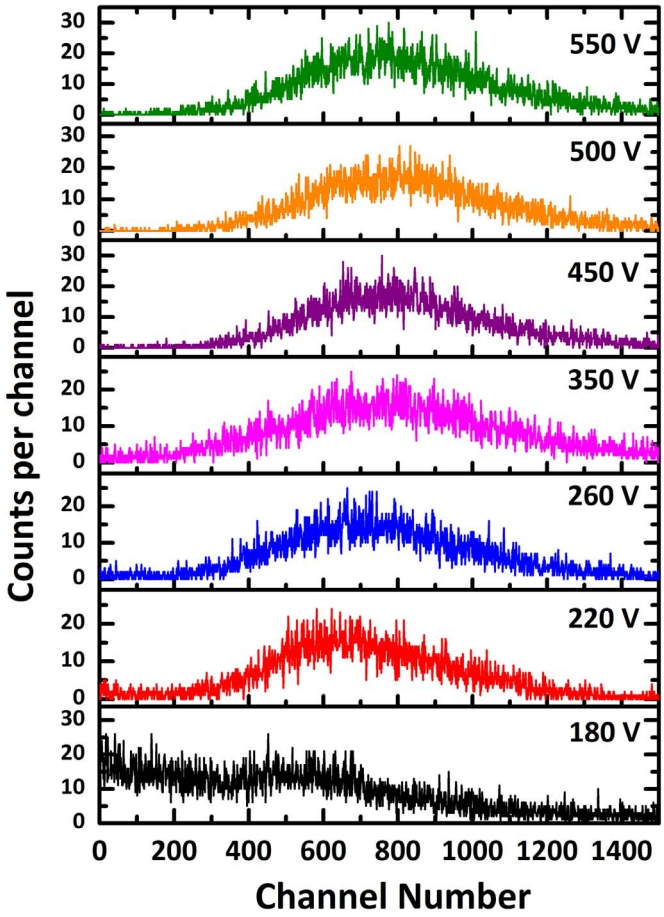

Fig. 4. Alpha spectra of ^{241}Am obtained after applying various voltages to the $MAPbBr_3$ single-crystal detector.

maximum voltage of 200 V (all experiments were conducted in air under dark conditions). The obtained linear curve (Fig. 3) exhibited a bulk resistor-type behavior. The dark current density was maintained at a constant level of 206 ± 10 nA/cm^2 even after applying a voltage of 200 V, owing to the large bandgap (Eg) of 2.3 eV. However, the latter also resulted in a relatively high empirical pair creation energy (W-value) of 6.03 eV, which was calculated using the formula W=2Eg +1.43 [19]. The slope of the fitting curve was used to estimate the detector resistivity, which was equal to $(7.8 \pm 0.2)\times10^{10}$ Ω cm at room temperature. The obtained high bulk resistance of the $MAPbBr_3$ single

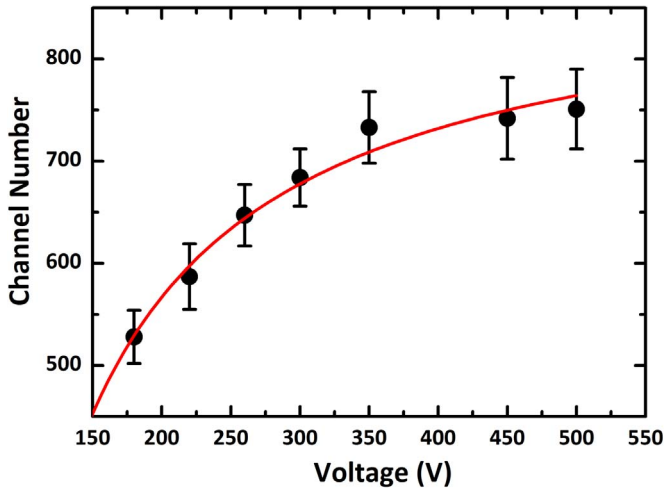

Fig. 5. Spectral peak centroids obtained at different applied voltages. The black circles represent the experimental data, which were fitted using the single-particle Hecht equation.

crystal allows extraction of the weak radiation signal and acquiring the energy spectra of alpha particles via event-by-event counting.

In this work, a series of the energy spectra of alpha particles were measured with the $MAPbBr_3$ single crystal detector under various voltages applied for 900 s (Fig. 4). The obtained spectra were generated under exposure to a 0.8 μCi ^{241}Am alpha source in air with a distance between the alpha source and the device at about 10 mm. In order to take into account the effects produced by energy losses and straggling of alpha particles in air, the TRIM software was used to simulate the measured alpha particle energy and peak broadening observed after traveling a 10 mm air gap. The conducted simulations yielded the energy loss of about 0.92 MeV and spectral peak broadening corresponding to an increase in its full width at half maximum (FWHM) of 56 keV. To verify that the ionization of air did not affect the measured alpha spectrum (due to possible collection of electron-ion pairs by the wires attached to the device), the utilized Cu wires were directly exposed to the same alpha radiation. The obtained results indicate no additional peak formation due to air ionization.

Although alpha particles supplied a fixed amount of energy to the detector, the collected charge was voltage-dependent. Fig. 5 shows the positions of the alpha peak centroids plotted at different applied voltages. Starting at 180 V, a weak peak was clearly observed, and its centroid shifted to higher energies with increasing electric field due to a more complete charge collection. The product of the charge carrier mobility (μ) and charge carrier lifetime (τ), which can be computed using the Hecht equation, is one of the most important detection parameters that allows determination of the average carrier drift distance per electric field unit and characterizes the performance of a semiconductor radiation detector [17]. Since the $MAPbBr_3$ single crystal consists of a hole-dominant material [18], the utilized Hecht equation can be written for the single-polarity charge transport as follows [20,21]:

$$Q(V) = \frac{\mu\tau N_0 qV}{L^2}[1 - \exp(\frac{L^2}{\mu\tau V})]$$

Here N_O is the number of electron-hole pairs generated by alpha particles, Q is the total number of collected holes, L is the thickness of the $MAPbBr_3$ single crystal, V is the applied voltage, and $\mu\tau$ is the mobility-lifetime product. The latter can be calculated by fitting the data depicted in Fig. 4 with the equation described above, assuming that the position of the peak centroid channel is proportional to the collected charge, and that the shaping times are much larger than the electron drift times. The obtained fitting parameters yielded the $\mu\tau$ hole product in a range $(0.4–1.6)\times10^{-3}$ cm^2/V. It should be noted that the fitting procedure based on the Hecht equation alone can result in large deviations of the calculated $\mu\tau$ magnitude [22]. In some cases, the computed $\mu\tau$ product underestimated the true μτ value due to ballistic deficit and surface trapping. The non-uniformity of the applied electric field (especially to a large planar detector with a point contact) also can significantly affect the resulting $\mu\tau$ product.

In conclusion, it was shown in this study that a bulk $MAPbBr_3$ single crystal was capable of detecting heavy ions. In particular, a charged particle radiation detector was built from a $MAPbBr_3$ single crystal with the MSM structure and dimensions of 5 mm×5 mm ×2 mm. Using the 0.8 μCi ^{241}Am alpha source, the dark current density was maintained at a level of 206 ± 10 nA/cm^2, and the obtained crystal resistivity was equal to $(7.8 \pm 0.2) \times10^{10}$ Ω·cm even at an applied voltage of as high as 200 V. The measured alpha energy spectra depended on the applied voltage, while the calculated hole mobility-lifetime product was $(0.4–1.6)\times10^{-3}$ cm^2/V.

Acknowledgment

The work was supported by the U.S. Defense Threat Reduction Agency (grant number HDTRA1–14–1–0030).

References

[1] Glenn F. Knoll, Radiation Detection and Measurement, John Wiley & Sons, 2010.
[2] G. Lutz, Semiconductor Radiation Detectors, Springer, Berlin, 1999.
[3] Brian D. Milbrath, J. Peurrung Anthony, Mary Bliss, William J. Weber, Radiation detector materials: an overview, J. Mater. Res. 23 (10) (2008) 2561–2581.
[4] T.E. Schlesinger, J.E. Toney, H. Yoon, E.Y. Lee, B.A. Brunett, L. Franks, R.B. James, Cadmium zinc telluride and its use as a nuclear radiation detector material, Mater. Sci. Eng. R–Rep 32 (2001) 103–189.
[5] R.C. Whited, M.M. Schieber, Cadmium telluride and mercuric iodide gamma radiation detectors, Nucl. Instrum. Methods 162 (1979) 113–123.
[6] T. Onodera, K. Hitomi, T. Shoji, Spectroscopic performance and long-term stability of thallium bromide radiation detectors, Nucl. Instrum. Methods Phys. Res. A 568 (2006) 433–436.
[7] D. Shi, V. Adinolfi, R. Comin, M. Yuan, E. Alarousu, A. Buin, Y. Chen, S. Hoogland, A. Rothenberger, K. Katsiev, Y. Losovyj, Low trap-state density and long carrier diffusion in organolead trihalide perovskite single crystals, Science 347 (2015) 519–522.
[8] Q. Dong, Y. Fang, Y. Shao, P. Mulligan, J. Qiu, L. Cao, J. Huang, Electron-hole diffusion lengths > 175 μm in solution-grown CH3NH3PbI3 single crystals, Science 347 (2015) 967–970.
[9] E.I. Wei, X. Ren, L. Chen, W.C. Choy, The efficiency limit of $CH_3NH_3PbI_3$ perovskite solar cells, Appl. Phys. Lett. 106 (2015) 221104.
[10] J.H. Im, I.H. Jang, N. Pellet, M. Grätzel, N.G. Park, Growth of $CH_3NH_3PbI_3$ cuboids with controlled size for high-efficiency perovskite solar cells, Nat. Nanotechnol. 9 (2014) 927–932.
[11] J. Wang, N. Wang, Y. Jin, J. Si, Z.K. Tan, H. Du, L. Cheng, X. Dai, S. Bai, H. He, Z. Ye, Interfacial control toward efficient and low-voltage perovskite light-emitting diodes, Adv. Mater. 27 (2015) 2311–2316.
[12] S.D. Stranks, H.J. Snaith, Metal-halide perovskites for photovoltaic and light-emitting devices, Nat. Nanotechnol. 10 (2015) 391–402.
[13] Y. Fang, Q. Dong, Y. Shao, Y. Yuan, J. Huang, Highly narrowband perovskite single-crystal photodetectors enabled by surface-charge recombination, Nat. Photonics 9 (2015) 679–686.
[14] S. Yakunin, M. Sytnyk, D. Kriegner, S. Shrestha, M. Richter, G.J. Matt, H. Azimi, C.J. Brabec, J. Stangl, M.V. Kovalenko, W. Heiss, Detection of X-ray photons by solution-processed lead halide perovskites, Nat. Photonics 9 (2015) 444–449.
[15] M.D. Birowosuto, D. Cortecchia, W. Drozdowski, K. Brylew, W. Lachmanski, A. Bruno, C. Soci, X-ray scintillation in lead halide perovskite crystals, Sci. Rep. 6 (2016) 37254.
[16] W. Heiss, C. Brabec, X-ray imaging: perovskites target X-ray detection, Nat. Photonics 10 (2016) 288–289.
[17] S. Yakunin, D.N. Dirin, Y. Shynkarenko, V. Morad, I. Cherniukh, O. Nazarenko, D. Kreil, T. Nauser, M.V. Kovalenko, Detection of gamma photons using solution-grown single crystals of hybrid lead halide perovskites, Nat. Photonics 10 (2016) 585–589.
[18] H. Wei, Y. Fang, P. Mulligan, W. Chuirazzi, H.H. Fang, C. Wang, B.R. Ecker, Y. Gao, M.A. Loi, L. Cao, J. Huang, Sensitive X-ray detectors made of methylammonium lead tribromide perovskite single crystals, Nat. Photonics 10 (2016) 333–339.
[19] Ram Devanathan, R. Corrales Louis, Fei Gao, William J. Weber, Signal variance in gamma-ray detectors—a review, Nucl. Instrum. Methods Phys. Res. A 565 (2) (2006) 637–649.
[20] K. Hecht, Zum Mechanismus des lichtelektrischen Primärstromes in isolierenden Kristallen, Z. Phys. 77 (1932) 235–245.
[21] P.J. Sellin, A.W. Davies, A. Lohstroh, M.E. Ozsan, J. Parkin, Drift mobility and mobility-lifetime products in CdTe: Cl grown by the travelling heater method, IEEE Trans. Nucl. Sci. 52 (2005) 3074–3078.
[22] K.A. Jones, A. Datta, K.G. Lynn, L.A. Franks, Variations in measurements in cadmium zinc telluride, J. Appl. Phys. 107 (2010) 123714.